DOI 10.1002/ejlt.200501010 *Eur. J. Lipid Sci. Technol.* **107** (2005) 594–606

Daniel Kalnin[a, b]
Pierre Lesieur[c, d]
Franck Artzner[a]
Gerard Keller[a]
Michel Ollivon[a]

[a] Equipe Physico-Chimie des Systèmes Polyphasés, UMR 8612 CNRS, Châtenay-Malabry, France
[b] Programme ACTIA 99/05, ADRIA Quimper, Créac'h Gwen, Quimper, France
[c] Laboratoire pour l'Utilisation du Rayonnement Electromagnétique, Université Paris-Sud, Orsay, France
[d] Laboratoire de Physico-Chimie des Colloïdes, UMR 7565 CNRS, Faculté des Sciences, Vandoeuvre-lès-Nancy, France

Systematic investigation of lard polymorphism using combined DSC and time-resolved synchrotron X-ray diffraction

The polymorphic behavior of lard was systematically investigated by differential scanning calorimetry (DSC) while simultaneously monitoring the formation of the different crystal forms with X-ray diffraction (XRDT). To interpret the complex polymorphic evolution of the sample analyzed by regular DSC, both XRD patterns and DSC curves were recorded at the same time from the same sample (20 mg) using a laboratory-made calorimeter (http://www.umr-cnrs8612.u-psud.fr/Francais/pdf/MICROCALIX.pdf) installed at a synchrotron radiation bench capable of both small- and wide-angle X-ray diffraction and time-resolved experiments. Lard exhibits a large melting range ($-30\,°C \leq T \leq 50\,°C$) with three main crystallization peaks. In this range, lard polymorphism was investigated by varying the cooling and heating rates between 10 and 0.15 K/min, and by isothermal recrystallization at -10 and 15 °C. XRD lines observed by SAXS at about 35, 43.8 and 48.2 Å are identified to subcells α, β'_1, β'_2 and β, and attributed to the main DSC peaks. The crystalline forms appearing during the cooling depend on the cooling rate and on the final temperature. Higher cooling rates lead to unstable α forms that transform subsequently upon heating and/or storage into β' forms. The persistence of a monotropic transformation at $-10\,°C$ that was monitored during isothermal storage is explained by the presence of a liquid phase at this temperature.

Keywords: Crystallization kinetics, DSC/XRDT, lard polymorphism, phase transition, storage conditions, structure, synchrotron radiation, TAG.

1 Introduction

Meat production from pigs was estimated at about 93 MT in 2001, from which about 50% and 22% were produced in China and Europe, respectively. Pork represents almost 40% of the world-wide daily meat protein intake. Lard is the fat obtained by rendering fatty tissue of the hog, the domestic pig. Natural lard has a characteristic waxy texture and exhibits unsatisfying bakery qualities, which are frequently corrected by fat blending or interesterification in making commercial shortenings [1–4]. Recently published studies concerning lard focus mostly on composition and analysis of genuine or modified lard [5–10]. The composition of lard varies with the hog's food [11–13] and mainly comprises a few long-chain major fatty acids which are about C16 24%, C18 14%, C18:1 41%, C18:2 10% [13]. Contrary to what is found for other fats, oleic acid is mostly found in the 1- and 3-position of glycerol, while palmitic acid is mostly esterified in the 2-position. Then, the 2-palmitooleostearin (PSO) and 2-palmitodiolein (OPO) are the major triacylglycerols (TAG) of lard, with about 13% and 19%, respectively [13]. The amount of the major trisaturated triacylglycerol, 2-palmitodistearin (SPS), is highly variable (2–10%). Although composed of only a few TAG, lard, as many other fats, exhibits complex thermal properties [6–10, 14, 15]. Indeed, when differential scanning calorimetry (DSC) is used for the investigation of the thermal properties of fats, often several peaks are observed on heating and cooling of samples. These DSC peaks reflect the occurrence of numerous thermal transitions, the temperatures and enthalpies of which vary as a function of sample thermal history [16–19] This complexity, which is also related to the fat composition, is drastically enhanced by the existence of a polymorphism of monotropic type for each single TAG [18, 20–24]. For instance, up to six crystalline forms have been evidenced for monounsaturated triacylglycerols such as POP [23–26]. However, the identification of the polymorphic forms of pure TAG does not allow the straight forward interpretation of complex DSC recordings [2, 5–

Correspondence: Daniel Kalnin, Food Physics Group, Agrotechnology and Food Sciences Group, Wageningen University, Bomenweg 2, NL-6703 HD Wageningen, The Netherlands. Phone: +31 317 483225, Fax: +31 317 483669, e-mail: daniel.kalnin@web.de

10, 14, 15]. Thus, identification of the species, the domain of existence of which is delimited by each melting or crystallization DSC peak, is rather complicated and often quite impossible without the help of techniques that yield information about structures (*e.g.* X-ray or neutron diffraction, infrared spectroscopy, *etc.*) [16–24]. Correct interpretation of both the diffraction patterns and the thermal analysis recordings requires that structural information obtained at different temperatures are compared [16–24]. The complementarity of these techniques and the necessity of such coupling and quantitative analysis for the study of thermal properties of fats have not yet been denied. Recently, a new instrument, equipped with Peltier-effect controlled sample holders, allowing DSC recordings simultaneously with synchrotron X-ray diffraction as a function of temperature (XRDT), has been used to study the thermal and structural properties of cocoa butter and milk fat [16, 17] (see also http://www.umr-cnrs8612.u-psud.fr/Francais/pdf/MICROCALIX.pdf). This setup allows the simultaneous comparison of three signals, which help to interpret the thermal events. While DSC curves provide information about the temperatures and enthalpies of thermal events, both small- and wide-angle XRDT, by the absence or presence of a set of diffraction lines, permit to identify and monitor changes of crystalline species even in very diluted systems [19]. Small-angle XRD (SAXS) peaks reflect the so-called long spacing (LS) and provide information about the longitudinal packing of the molecules [27, 28]. Wide-angle XRD (WAXS) monitors the diffraction peaks reflecting the lateral organization of the chains (short spacing, SS) [27, 28]. For TAG, the LS correspond frequently to 2, 3, sometimes 4 or 6, fatty chains, which are stacked in a parallel fashion, one on top of the other, in one crystal cell unit. LS depends on the length of the chains, their ability to pack together and the presence of "potential defects of packing", such as unsaturations or ramifications, along the chains [18, 23, 28]. More than three crystalline subcells have been identified in the WAXS patterns of TAG, depending on the sample's thermal history and also on the unsaturated fatty chains. This fact makes interpretation difficult, especially at low temperatures, at which all TAG are nearly crystalline and because diffracted peaks are overlapping [18, 29]. First attempts to characterize thermal and structural behavior of lard using DSC, XRD and/or pulsed NMR [5–10, 16, 29] are already published. However, none of these studies provides the comprehension of both thermal and structural properties of lard. This paper represents a systematic study of the thermal and structural behavior of lard. Combined DSC and time-resolved XRDT using synchrotron radiation on the high resolution bench D22 at L.U.R.E. has been chosen for our investigation because of its resolution at small angles. The effects of cooling and heating rates on the formation of the various crystalline species were studied in the range of 0.15–10 K/min. Phase transitions were also observed during isothermal conditioning at low temperatures.

2 Materials and methods

2.1 Lard sample preparation

Lard was provided by Luissier Bordeau Chesnel (Changé, Champagne; France). Samples were heated to 70 °C, homogenized and divided into aliquots of smaller quantities to be analyzed as received. When not specified differently, the thermal history of all samples was systematically annihilated by heating them for about 10 min to at least 10 K above their final melting point ($\geq$70 °C).

2.2 DSC

Thermal analysis was performed using a DSC 7 (Perkin Elmer) equipped with a cooling device (Intracooler II) supported by Pyris Thermal Analyzing Systems version 3.52. Recordings were obtained by measuring the heat transfer either by cooling or heating at constant rates or in isothermal mode. All samples, in the range of 10–15 mg, were introduced and sealed in 50-μL aluminum pans (pans B014–3017 and covers B014–3003; Perkin Elmer) and stored at room temperature ($\sim$22 °C). The instrument was standardized for all cooling and heating rates applied using the enthalpy and melting point of lauric acid [30]. An empty sealed pan (same as above) was used as reference. The analysis of lard was accomplished in the range of –50 °C $\leq$ T $\leq$ 70 °C. For the DSC curves, the onset and the peak maximum were determined using standard analyzing routines (see Fig. 1).

2.3 XRD as a function of temperature combined with DSC (DSC/XRDT)

XRD patterns were recorded with synchrotron radiation on the high-resolution beam line (D22) of L.U.R.E. The X-ray wavelength used was 1.549 Å (8 keV). The X-ray pattern acquisition time varied between 60 and 300 s per frame (according to the different heating and cooling rates). XRD patterns were measured in the range of -20 °C $\leq$ T $\leq$ 60 °C. The specifications and capabilities of the calorimeter used, equipped with Peltier-effect controlled sample holders, have been published [16, 17]. Briefly, two position-sensitive gas-filled linear detectors were used simultaneously and placed at a sample-to-detector distance of 0.30 m for WAXS and 1.75 m for SAXS. This setup leads to XRD patterns corresponding to 0.005 Å^{-1} $\leq$ q $\leq$ 0.40 Å^{-1} for SAXS and about

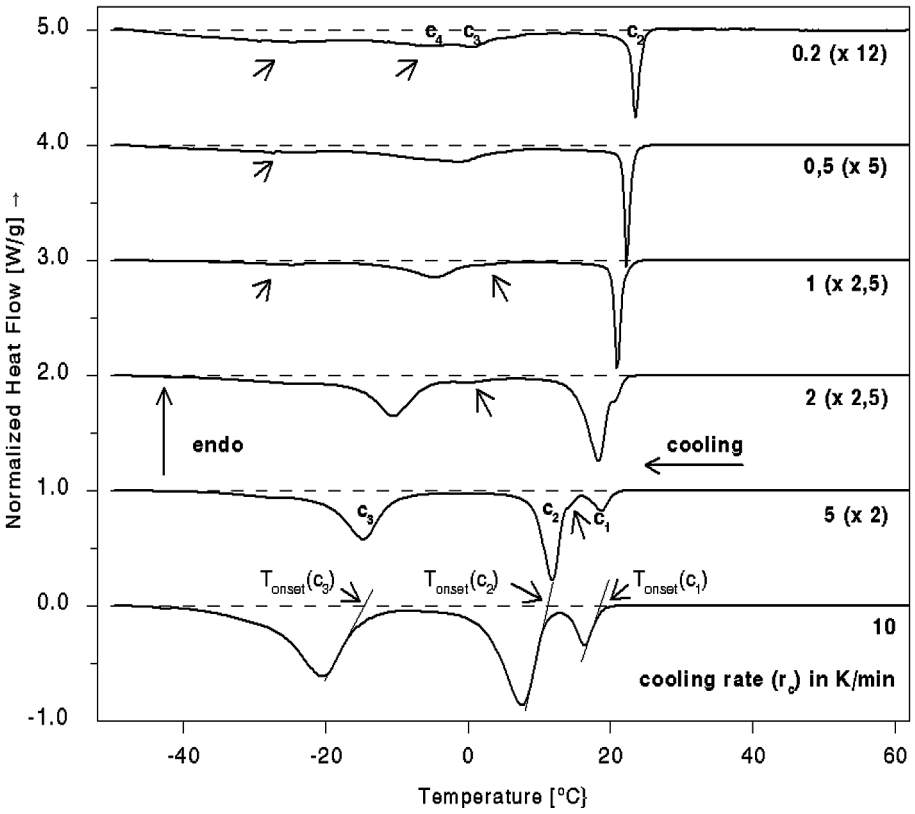

Fig. 1. Characteristic DSC curves representing the crystallization of lard. The influence of the cooling rate (r_C) is evidenced in the range of –0.2 K/min up to –10 K/min, as indicated. The normalized heat flow is scaled to the cooling rate of –10 K/min. DSC curves are shifted relatively to each other and multiplied for clarity as indicated in brackets. When not associated to T_{Onset}, arrows indicate minor exothermic events. Thermic events are specified, when applicable, to major thermic events abbreviated as c_i (cf. Tab. 1).

Tab. 1. Crystallization and melting enthalpies of lard. The crystallization and melting enthalpies ΔH and T_{Onset} of lard as deduced by a DSC 7 for the different thermal events. Cooling rates r_C varied from −0.2 K/min to −10 K/min. Heating was performed at one heating rate r_H = 5 K/min (according to Figs. 1 and 2).

r_C [K/min]	c_1		c_2		c_3		$c_1+c_2+c_3$
	ΔH_2 [J/g]	T_{Onset} [°C]	ΔH_3 [J/g]	T_{Onset} [°C]	ΔHC [J/g]	T_{Onset} [°C]	ΔH_1 [J/g]
0.2	4.0	65.5	25.6	29.8			95.3
0.5	4.0	54.2	24.2	36.5			90.7
1.0	1.8	53.4	23.0	34.1			87.5
2.0	− 5.6	49.7	21.2	35.1			84.9
5.0	− 9.3	45.2	15.2	31.1	22.2	5.4	81.8
10.0	−13.4	37.8	12.8	32.5	20.2	5.9	76.32
r_H = 5 K/min (after 1 min at 50 °C) and cooling at r_C [K/min]	$h_{6,7}$		$h_{3,4,5}$		$h_{1,2}$		$h_{6,7} + h_{3,4,5} + h_{1,2}$
	$\Delta H_{6,7}$ [J/g]	T_{Onset} [°C]	$\Delta H_{3,4,5}$ [J/g]	T_{Onset} [°C]	$\Delta H_{1,2}$ [J/g]	T_{Onset} [°C]	ΔH_H [J/g]
0.2	55.4	−10	24.4	21	8.2	36	88
0.5	50.8	−12	28.6	19	6.6	37	85.8
1.0	49	−15	32.6	18	5.4	38	87
2.0	43.4	−15	34.8	16	4	40	82.2
5.0	44	−15	41	14.5	0.2		85
10.0	35.6	−22	46.8	12	0.1		82.6

$1\ Å^{-1} \leq q \leq 2\ Å^{-1}$ for WAXS. This is referring to plane spacing (d) $125\ Å \leq d \leq 15\ Å$ and $6.3\ Å \leq d \leq 3.1\ Å$, respectively. A single computer was used for simultaneous SAXS, WAXS and DSC data collection in order to avoid temperature and/or time lags between recordings, thanks to a Visual Basic program written by P. Lesieur. X-ray calibration was obtained at 20 °C with the stable β-modification of ultra-pure SSS [20] and silver behenate [31] (they perfectly agree). DSC calibration was performed as above. Lard samples were introduced in thin (0.01 mm wall thickness, Ø ≤1.5 mm) glass capillaries (GLAS; Müller, Berlin, Germany) with a syringe and/or by centrifugation (1000 rpm) at T ≥ 60 °C. So-prepared samples were stored at T = −30 °C and/or T = 4 °C and sealed by a drop of melted paraffin under argon atmosphere to avoid oxidation.

2.4 Crystallization as a function of cooling rate

Samples were cooled from 70 to −50 °C at cooling rates in the range of -0.2 K/min ≥ r_C ≥ –10 K/min. The crystallization was studied by DSC, and up to cooling rates of $r_C \geq$ –5 K/min with XRD.

2.5 Melting as a function of the cooling rate applied

Samples that were cooled by the above-mentioned method were kept for 1 min at T = −50 °C, then reheated at heating rates in the range of 0.2 K/min ≤ $r_H \leq$ 10 K/min. The heating was also studied by DSC/XRDT at heating rates up to $r_H \leq$ 5 K/min.

2.6 Isothermal crystallization as a function of time and temperature

2.6.1 DSC analysis

DSC 7 was also used to monitor the change occurring in lard samples quenched to $-15\ °C \leq T_{cond} \leq 20\ °C$ in steps of 5 K. Typically, samples were cooled at $r_C = -100$ K/min from 70 °C to T_{cond} and kept for various times, ranging from 0 to 10 min, at this temperature. Then, samples were rapidly heated at r_H = 10 K/min, to minimize further changes.

2.6.2 DSC/XRDT analysis

The same experimental setup was used to follow the structural changes occurring during isothermal conditionings at $T_{cond} = -10$ and 15 °C. Although the capillary containing the melted sample was rapidly introduced into the precooled calorimeter (quenching is about 2 s), due to the limitations of the apparatus, diffraction patterns could only be recorded after about 60 s. DSC was recorded simultaneously with XRD. Scattering was recorded for 30 min (60 s per pattern). Each isothermal conditioning was followed by a DSC/XRDT recording at r_H = 2 K/min.

3 Results and discussion

3.1 DSC analysis

A lard sample has been systematically analyzed by DSC as a function of heating (r_H) and of cooling rate (r_C), then by DSC/XRDT using synchrotron radiation. The influence of cooling and heating rates upon the lard physical properties was first studied by DSC at all 36 combinations of the six rates used in the range of –0.2 K/min ≤ $r_C \leq$ –10 K/min. A selection of the thermal recordings obtained is presented here, together with an interpretation of the origin of the transitions thanks to the coupled time-resolved synchrotron DSC/XRDT analysis.

3.1.1 Crystallization as a function of r_C

The crystallization of lard samples was studied from T = 70 to −50 °C as f(r_C) using DSC as described above. The recordings obtained at the six different r_C are presented (Fig. 1). The comparison of these recordings shows that (i) the DSC cooling curve of lard strongly depends on the cooling rate, (ii) at least three major peaks can be distinguished, denoted c_1 to c_3 in the order of decreasing temperature, and (iii) the onset temperature (T_{Onset}) of lard crystallization decreased from 25.6 °C to 20.2 °C with decreasing r_C (Tab. 1). In addition, it has been observed that the total enthalpy of crystallization decreased with decreasing r_C (Tab. 1). Peak c_1 apparently disappeared or merged with c_2 at $r_C \leq$ –1 K/min. It is worth noting that this merging results from the fact that c_1 and c_2 exotherms display very different temperature dependencies. Such T dependence is even stronger for c_3 since it increased its maximum temperature from −18.6 °C to 1.6 °C with decreasing r_C. In fact, crystallization is even more complex. At r_C = –1 K/min, up to five peaks can be distinguished (arrows in Fig. 1), showing that more than three stable crystalline organizations are obtained at lower temperatures and/or after longer times.

3.1.2 Melting as a function of r_C

Samples that were crystallized at the above cooling rates were kept for 1 min at T = −50 °C, then heated at all rates indicated, corresponding to 36 recordings in the range of 0.2 K/min ≤ $r_H \leq$ 10 K/min. Only the recordings corresponding to r_H = 5 K/min are shown in Fig. 2. As for the

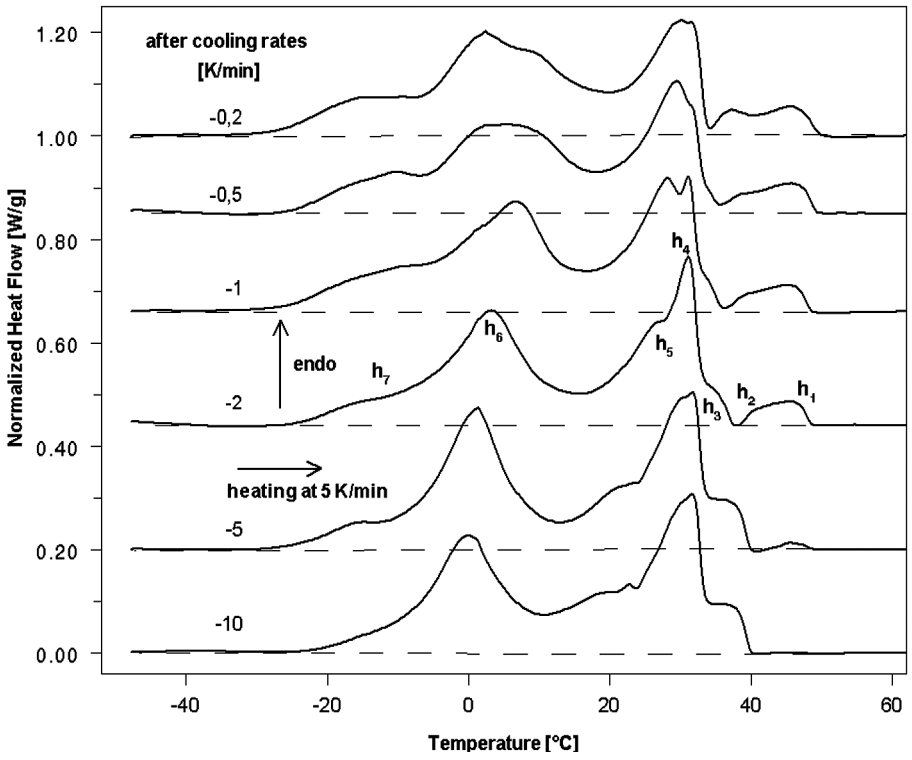

Fig. 2. Characteristic DSC heating curves for lard heated at r_H = 5 K/min following a cooling from 70 to −50 °C and an isotherm of 1 min at −50 °C at different cooling rates varying from –0.2 K/min to –10 K/min, as indicated. DSC curves are shifted as in Fig. 1. Thermic events are specified, when applicable, to major thermic events abbreviated as h_i (cf. Tab. 1).

influence of the cooling rate, it has been observed that (i) the transitions observed in the DSC heating curves recorded at the same r_H (here r_H = 5 K/min) depend on the former r_C applied, (ii) the 36 DSC heating recordings obtained by varying both r_C and r_H show that they always depend on both cooling and heating rates (data not shown), and (iii) up to seven endothermic peaks named from h_1 to h_7 can be distinguished.

The first endothermic effect appeared at approximately T = −30 °C; in fact, in the range of −30 and −20 °C, depending on r_C. Two main melting endotherms, the temperature positions of which are quite varying, are observed around 0 and 30 °C, respectively (Fig. 2). At r_C = –5 K/min, two overlapped endotherms h_1 and h_2, the importance of which increases with decreasing r_C, are only recorded at T >40 °C. Such endotherms, which are mainly observed at $r_C \leq$ –5 K/min, should correspond to the formation of stable varieties. Their final melting points increase with decreasing cooling rates from about 45 to 51 °C. At r_C = –5 K/min, their enthalpies are very low, showing that the formation of these stable forms is far from being complete (Tab. 1). The enthalpy of the h_3 endotherm decreased with decreasing r_H and disappeared at r_H <0.5 K/min. We interpreted the decrease of the h_3 endotherm *vs.* r_C as corresponding to the formation of an unstable variety yielding h_1 and h_2 at the lowest r_C and/or after longer time (see below, cf. Fig. 6).

3.2 X-ray analysis

Coupled time-resolved XRDT and DSC was used for the identification of the species formed during most of the r_C and r_H at $r_C \approx r_H$. However, due to the apparatus limitations, lard crystallization was only investigated at $r_C \leq$ 5 K/min, and X-ray scattering has only been measured between −20 °C ≤ T ≤ 60 °C; so the full crystallization of lard could not be obtained at r_C >0.3 K/min (cf. Ref. [2, 8]). Only the results corresponding to boundary conditions (5 K/min and 0.3/0.15 K/min) will be presented below.

3.2.1 Fast cooling and heating

Fig. 3A and B show SAXS and WAXS X-ray pattern evolution during a fast crystallization at r_C = −5 K/min followed by a melting at r_H = 5 K/min. The DSC recordings shown in Fig. 3C are nearly the same as obtained for the same r_C and r_H recorded with DSC 7, so we kept below the same DSC peak notations as above. The central scattering is strongly increasing while the first diffraction peak can be monitored, which is due to the occurrence of small crystals. At this rate, a first SAXS peak (48.2 Å) can be observed at T <19.2 °C (c_1) (Fig. 3A). A second diffraction peak (35.1 Å) appeared at T <13.9 °C (c_2). From T < −12.7 °C, a dominant diffraction peak appeared at 43.8 Å

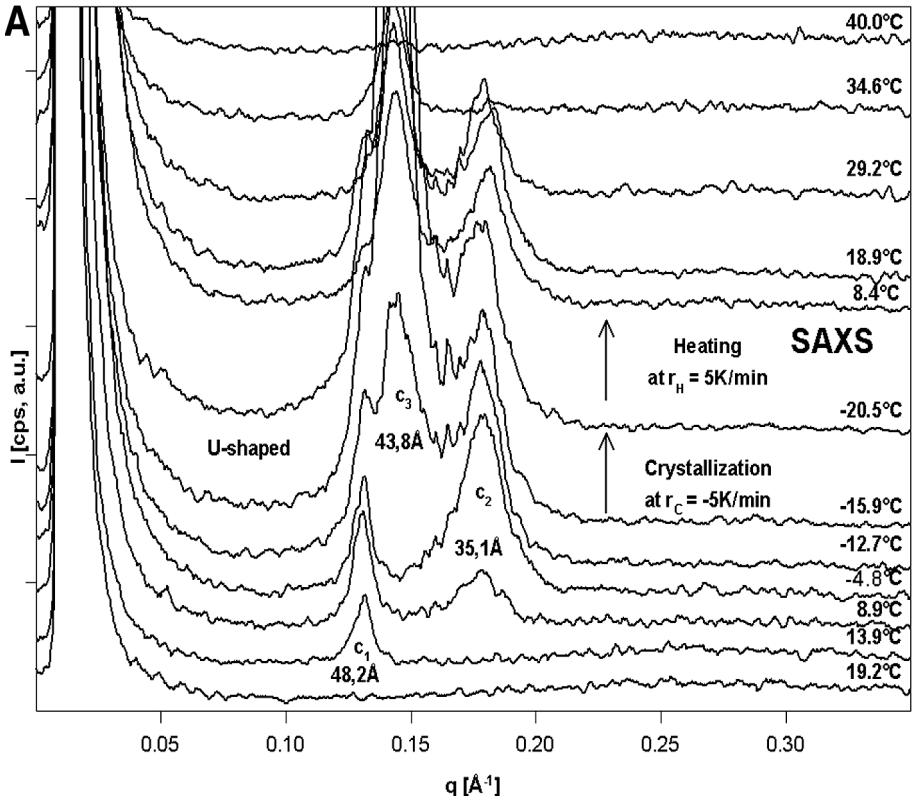

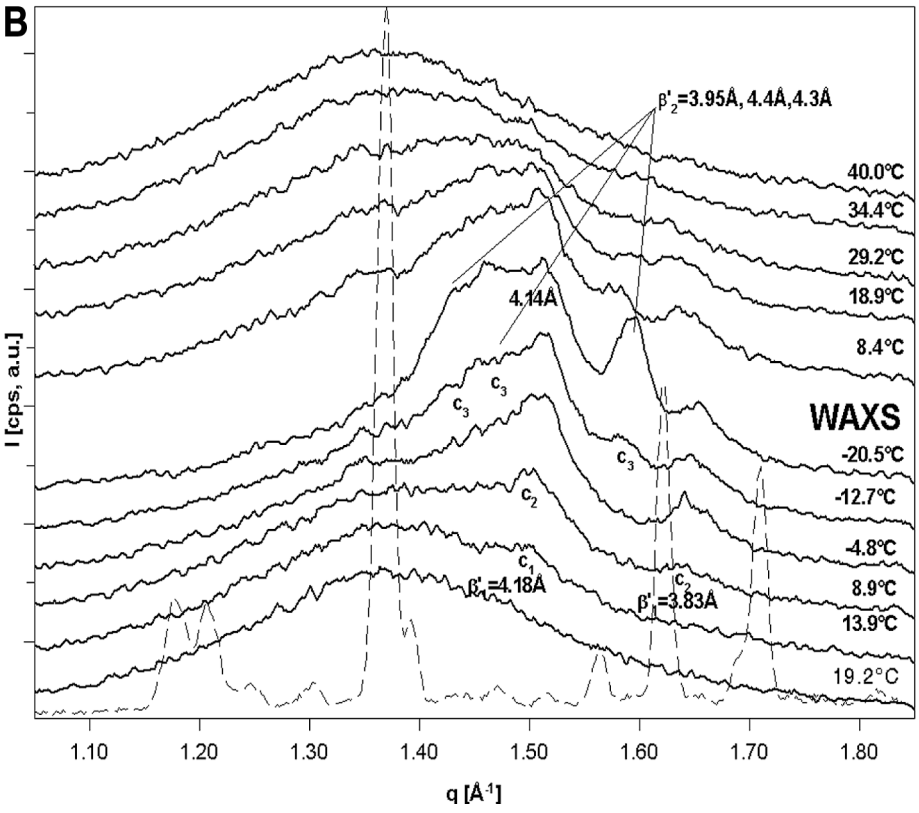

Fig. 3. Continued on next page.

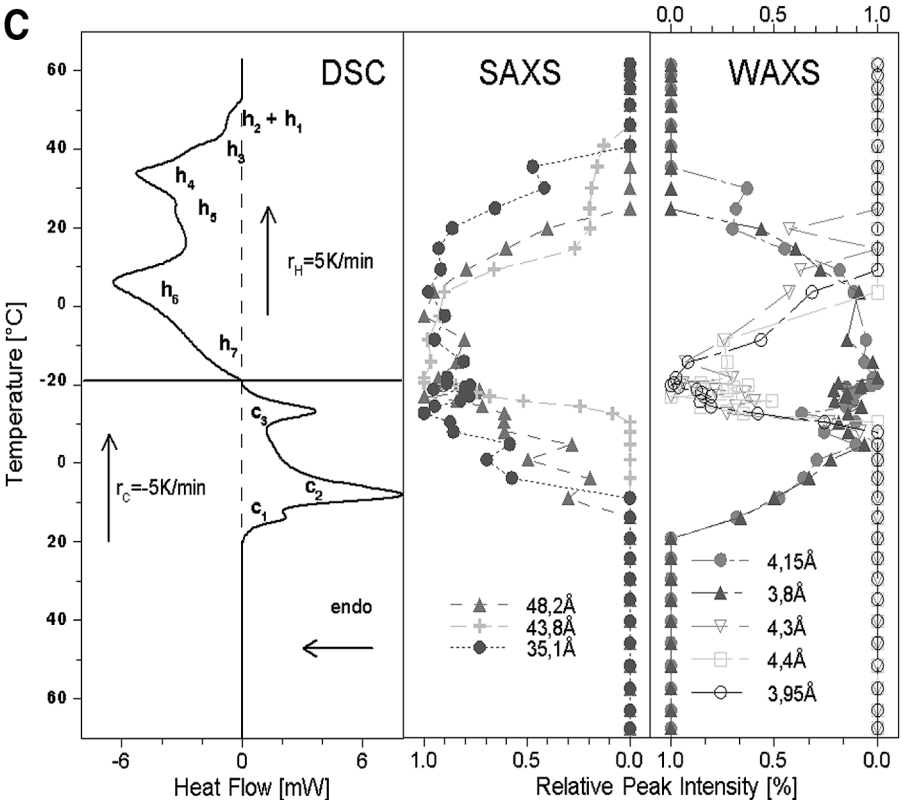

Fig. 3. Characteristic XRD patterns and DSC recordings obtained during the same experiment and for the same sample using synchrotron radiation for fast crystallization of lard at r_C = –5 K/min followed by fast heating at r_H = 5 K/min. Major thermic events are specified according to Tab. 1 as h_i and c_i. (**A**) Selection of SAXS patterns at the average temperature indicated. (**B**) Corresponding WAXS patterns. The WAXS pattern of pure tristearin (SSS) is shown for comparison (dashed line). All X-ray patterns were recorded for 60 s and shifted relatively to each other for clarity. (**C**) The corresponding DSC curves are drawn for comparison next to the SAXS and WAXS relative peak intensity plots *vs.* T. Evolution of three SAXS and five WAXS lines is followed and plotted with normalizations on the peak maximum intensity.

(c_3). Three SAXS peaks can be identified to the three main DSC peaks recorded simultaneously (denoted above as c_1 to c_3). The main diffraction lines of the various species observed are presented in Tab. 2.

At T $\geq$19.2 °C, only a broad WAXS peak is observed at q = 1.37 Å^{-1}, signifying that the fatty acid chains are in the liquid state. On cooling, the first WAXS peak (4.2 Å) appeared simultaneously with DSC peak c_1 at T $<$19.2 °C and was attributed to the formation of some α form, thanks to the presence of a SAXS peak at 48.2 Å (Fig. 3A, B). In fact, the attribution of the crystallization to an α form rather than to a β' form is difficult and is only deduced from the value of the long spacing observed; taking into account the fatty acid and triacylglycerol compositions, a 48.2 Å value cannot correspond in lard to a tilted-chain β' form, but rather to an α form with vertical chains [27, 28]. The occurrence of both 4.18 and 3.83 Å peaks, indicative of a β' form recorded at T $<$13.9 °C, coincides with that of both the d = 35.1 Å SAXS peak and the exotherm c_2. The shift of both WAXS peaks to higher q as the temperature decreases is interpreted as a diminution of the crystalline subcell parameters. The correlation observed in their shifts shows the coupling of both peaks (see heating below). The occurrence of a SAXS peak at 35.1 Å together with that at 48.3 Å allowed the identification of the coexistence of two subcells, thanks to the high resolution of the D22 SAXS beam line. At T $\leq$ −12.7 °C, a series of three WAXS lines at 3.95, 4.3 and 4.4 Å, and one SAXS line at 43.8 Å corresponding to the crystallization peak c_3, indicate the formation of a new species. It is worth noting that, again, SAXS lines appeared subsequest to the DSC peak and the WAXS lines were observed soon after. This can be interpreted as a delay in the TAG layer organization after self-organization of the chains. In other words, methylene groups of the chains organize first, before the whole TAG molecules. However, as the sample was kept at −20 °C for several minutes, we observed that the WAXS lines substantially developed at this temperature, showing that at this cooling rate crystallization is incomplete (cf. Ref. [2, 8]). This is in line with the observation that at r_C = −5 K/min, all WAXS peaks are observed on the top of a broad scaltering "line" centered at q = 1.37 Å^{-1} (d = 4.6 Å), indicative for the presence of a rather high amount of liquid phase or disorganized structures. The WAXS pattern of the pure β form of tristearin is reported in Figs. 3B and 4B for comparison to that of lard. The presence of this "liquid" or "disordered" phase at −20 °C, probably related to the broad TAG composition (differences in chain length and unsaturation likely lead to a loose packing), explains the polymorphic changes observed above.

Tab. 2. Correlation DSC event-crystalline subcell. Main crystallographic parameters of the fat polymorphs in lard and their attribution to major DSC peaks.

Polymorph form (subcell)	**SAXS** peaks d [Å]	**WAXS** peaks d [Å]	DSC **exotherms**	DSC **endotherms**
α (hexagonal)	48.2	4.18	c_1	h_3
β'$_1$ (orthorhombic)	35.1	4.14, 3.83	c_2	h_4, h_5
β'$_2$ (pseudo-orthorhombic)	43.8	3.95, 4.4, 4.3	c_3	h_7, h_6
β (triclinic)	43.8	4.6	c_2 (only upon slow cooling rates)	h_1, h_2

Upon heating, in the range of −20 to 15 °C, the diffraction line at 43.8 Å, apparently coupled with those at WAXS 4.3, 4.4 and 3.95 Å, partly vanishes as shown in Fig. 3A and C during the corresponding h_6 and h_7 endotherms. Contrary to the diffraction line at 43.8 Å, the WAXS lines completely disappeared. The h_5 endotherm was related to the decreases of lines at 3.8 Å correlated with 48.2 Å in the range of 15 °C $\leq$ T $\leq$ 25 °C. The vanishing of the diffraction line at 35.1 Å coupled with that at 4.15 Å leads to the h_4 and h_3 endotherms, although this does not explain their occurrence. During the set of h_1 and h_2 endotherms (distinct in Fig. 5), only one SAXS diffraction line can be monitored to be still persistent at T $\geq$ 40 °C (Fig. 3C).

3.2.2 Slow cooling and heating

An example for the evolution of X-ray scattering at r_C = −0.15 K/min followed by a heating at r_H = 0.3 K/min is given in Fig. 4A and B. A first weak scattering peak (45.4 Å) can be distinguished at about 26 °C (data not shown). At 24 °C, this peak rapidly vanishes and splits into two weak peaks of longer (49.6 Å) and shorter distances (44.2 Å), respectively. Both peaks vanished within the 2 K scan, while a very broad and important scattering is observed at about q = 0.05 Å^{-1}. This effect can also be distinguished at r_C = 0.5 K/min (data not shown). The peak at the shorter distance progressively shifts to 43.8 Å. A broader scattering peak appeared at d = 34.7 Å from T = 22.7 °C, shifting to 34.3 Å at lower T. The intensity of the scattering at 43.8 Å rose strongly at T <6.5 °C, while a second-order peak is observed at 21.9 Å. It is worth noting that the half height widths of both SAXS peaks at 43.8 and 34.5 Å are very different; while the line at 43.8 Å is very sharp, the half width of the peak centered on 34.5 Å is about four times broader, indicating a highly disordered structure for the latter.

At wide angles, the scatterings of two apparently coupled peaks appear at 4.15 and 3.85 Å from T <22.7 °C (c_2), indicating the formation of a β' chain packing (Fig. 4C). Then, a line at 4.61 Å rose at 20.7 °C, showing the occurrence of some β packing. Another three peaks (4.4 and 4.3 and 3.95 Å) appeared separately at negative temperature. All six WAXS lines got very sharp, and their position and intensity was monitored *vs.* T. While the characteristic β' lines (3.8 and 4.14 Å) exhibit a strong positive linear T dependence of about 2% within 50 °C, the β line does not change its position. The dependence of the other diffraction peaks is more complex, since the line at 3.95 Å is reaching a maximum around 0 °C while the one at about 4.3 Å exhibits the reverse behavior and the 4.4 Å line is almost not changing. The behaviors of all six lines are reversible with T. The β lines, observed at 4.6 Å and around 3.9 Å, persist at T $\geq$ 37.8 °C, showing that the phase likely formed by trisaturated TAG is the most stable.

All data show that the crystalline structure strongly depends on the sample time and the temperature history. Several polymorphic forms of β and β' type, and possibly α type, are observed. The occurrence of these crystalline varieties depends on the cooling rate, showing that lard exhibits a strong polymorphism. The crystallization extending at T $\leq$ −20 °C and the enthalpies of the DSC peaks recorded demonstrate the existence of an important liquid phase together with the crystalline phases described above at least down to −20 °C (Fig. 1). While this liquid phase rapidly contributes to reaching the formation of stable varieties and thermodynamic equilibrium (Ostwald ripening), polymorphic transitions can be monitored even at fast scanning rates (about 5 K/min) using the brightness of synchrotron radiation.

To further evidence the polymorph changes that may occur during thermal treatment of lard, complementary isothermal conditionings were performed and recorded.

3.3 Isothermal conditionings

The transitions occurring during isothermal conditioning following rapid crystallization of lard were also monitored using both DSC and DSC/XRDT using synchrotron radia-

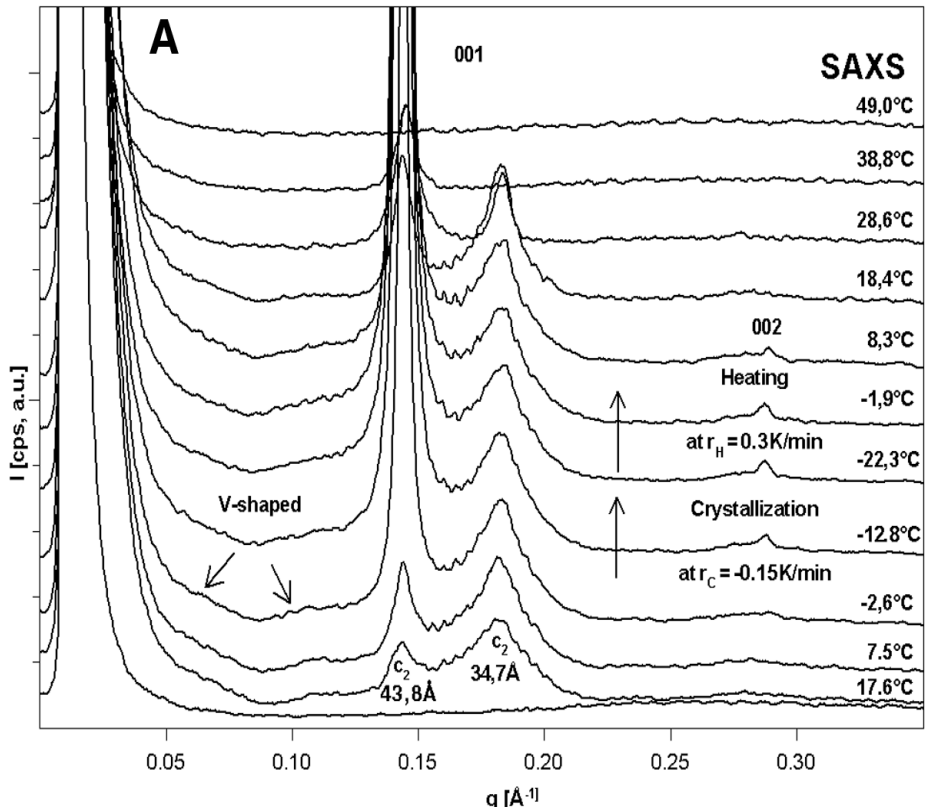

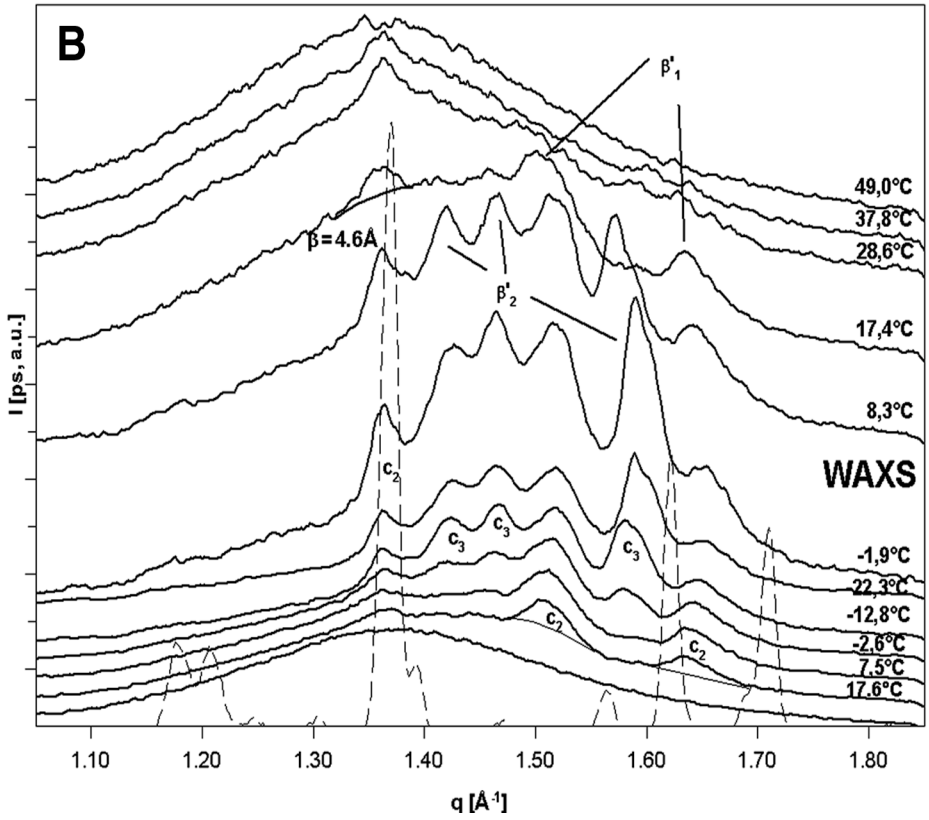

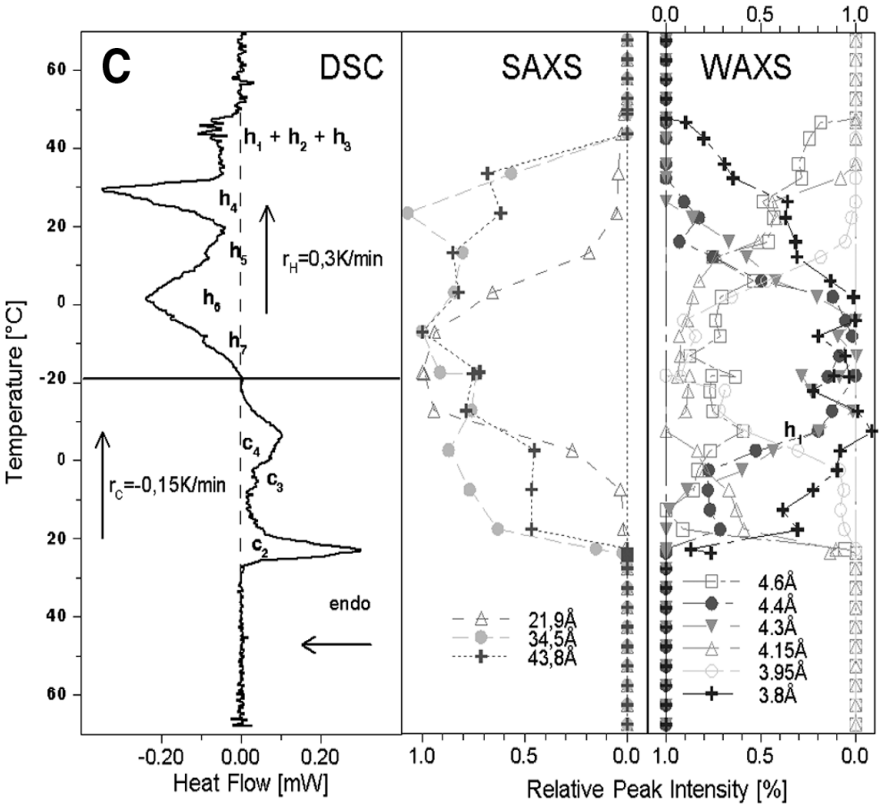

Fig. 4. Characteristic XRD patterns and DSC recordings obtained during the same experiment and for the same sample using synchrotron radiation for slow crystallization of lard at r_C = –0.15 K/min followed by slow heating at r_H = 0.3 K/min. Major thermic events are specified according to Tab. 1 as h_i and c_i. (**A**) Selection of small SAXS patterns at the average temperature indicated. Patterns were recorded for 400 s. (**B**) Corresponding WAXS patterns. The WAXS pattern of pure tristearin (SSS) is shown for comparison (dashed line). X-ray patterns were recorded for 200 s and shifted relatively to each other for clarity. (**C**) The corresponding DSC curves are drawn for comparison next to the SAXS and WAXS relative peak intensity plots *vs.* T. Evolution of three SAXS and five WAXS lines was followed and plotted with normalizations on the peak maximum intensity.

tion. Two types of isothermal conditioning are considered below: First, the heating following the isothermal conditioning is monitored by DSC, indirectly showing polymorphic transformation, and second, the isothermal transformation is monitored directly by DSC/XRDT.

3.3.1 DSC monitoring

The DSC recordings obtained after conditioning times ranging from t_{cond} = 0–10 min are shown in Fig. 5A, B. After t_{cond} = 0 min and isothermal conditioning at T_{cond} = 15 °C, almost no crystallization of stable species melting at $T \geq 30$ °C could take place, as shown by one single endotherm recorded at about 25 °C (Fig. 5A). Neither stable forms, such as h_1 or h_2, nor h_3 is formed. On the contrary, after 1 min of conditioning, h_3 and h_2 or h_1 endotherms are recorded in addition to the melting of unstable forms. Longer conditioning (2 and 10 min) leads to increasing $h_1 + h_2$ peaks. The same behavior is observed upon heating at r_H = 10 K/min after T_{cond} = –10 °C conditioning (Fig. 5B). A set of melting endotherms was always recorded, and the formation of some stable form was observed whatever the conditioning time was. Comparison of Fig 5A and B shows that with T_{cond} = 0 min, stable forms only crystallize at temperatures below 15 °C.

The endotherms h_1 and h_2, corresponding to the melting of stable varieties, increase in enthalpy as the conditioning time at 15 °C increases (Fig. 5A). Taking into account the fast scanning rates, especially upon heating, which further limit the evolution of the crystals, the comparison of the enthalpies of these peaks allows the determination of the crystallization rate of these varieties at 15 °C, which is $\delta H(h_{1,2})/\delta t = 0.66 \pm 0.02$ mJ g^{-1} min^{-1}.

Surprisingly, the amount of crystal formed shown by the enthalpies of the h_3 endotherm decreases with increasing conditioning time within 5 min at −10 °C, while the enthalpies of the h_1 and h_2 endotherms do not change considerably after t_{cond} = 1 min.

3.3.2 DSC/XRDT

Similar experiments were performed using DSC combined with synchrotron radiation XRD, as described in the Materials and methods section (only the isothermal conditioning at −15 °C is shown). Fig. 6 nicely illustrates the monitoring of the phase transition α to β' at T = −15 °C. A remarkable aspect of this phase transition is the persistence of the main line of the WAXS pattern at about 4.15 Å, which corresponds to both hexagonal and

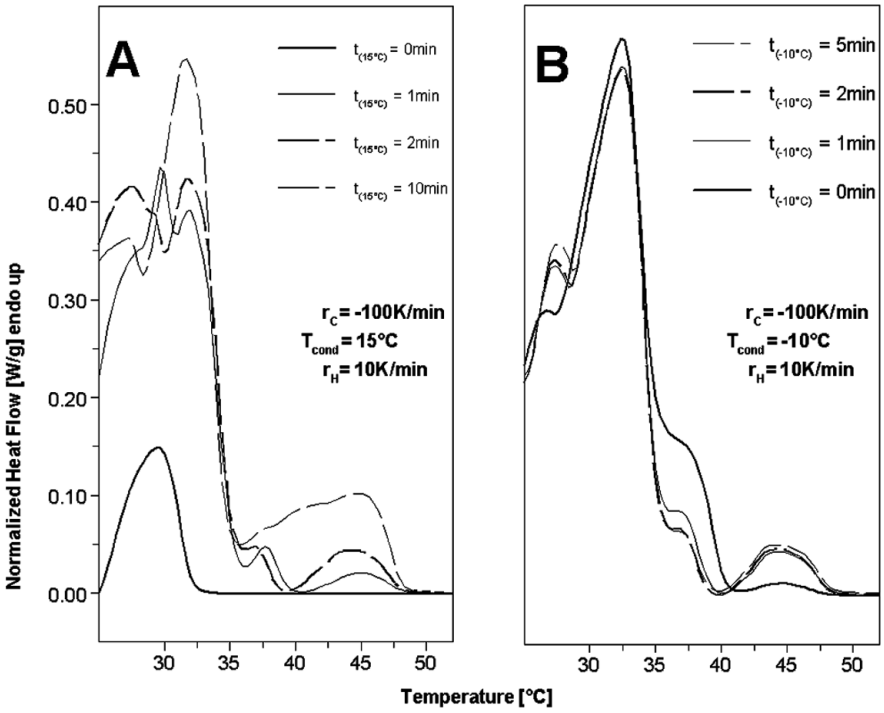

Fig. 5. DSC curves monitoring the consequence of isothermal conditioning at $T_{cond} = -10$ and 15 °C. The formation of various amounts of the high melting forms is evidenced in the DSC curves recorded on heating at r_H = 10 K/min following a fast cooling at r_C = 100 K/min from 70 °C to T_{cond} = 15 °C (**A**) and −10 °C (**B**). In this experiment, the conditioning time $t_{15\,°C}$ and $t_{-10\,°C}$ was varied between 0 and 10 min.

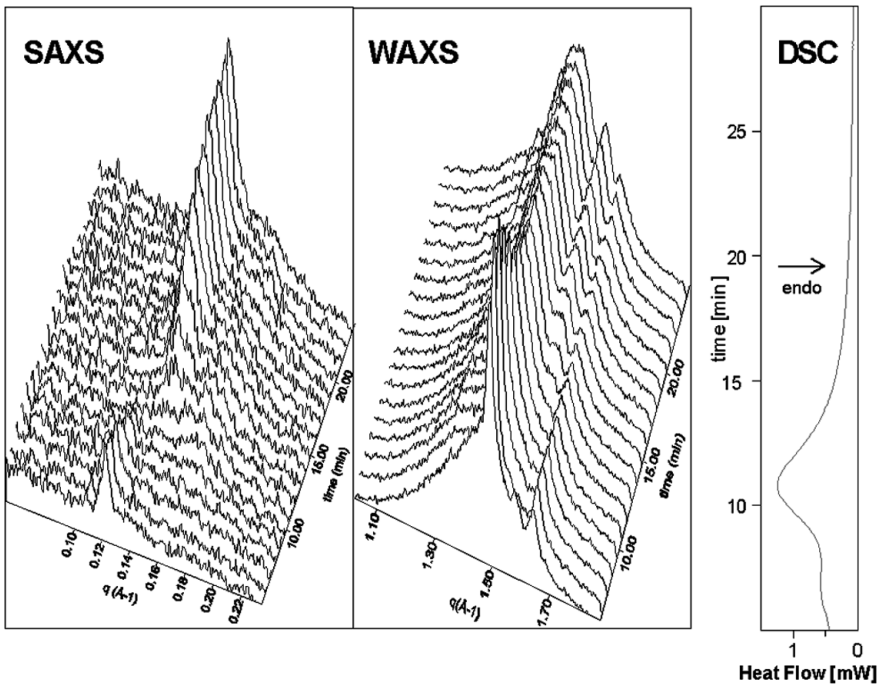

Fig. 6. Monitoring of the phase transitions occurring at $T_{cond} = -10$ °C after quenching of melted lard at about r_C = 2000 K/min. After quenching from about 70 °C to −10 °C, lard sample structural and thermal evolution was monitored by SAXS, WAXS and DSC during 30 min (5–25 min shown).

orthorhombic subcells, while that of the SAXS pattern at 48.2 Å vanishes at least for 1 min before that of 43.8 Å appears. This makes us conclude that during the transition corresponding to the change in chain tilt, the lateral order in the chain packing is at least partially maintained while the stacking order between lamellae is lost. The passage through an intermediate liquid crystalline-like state cannot be ruled out. During this transition, an exothermal process is recorded by DSC, the onset of which is at 8 min and its maximum is at about 11 min from the beginning of the isothermal experiment. This phase transformation process is extremely rapid and energetically "concentrated", there-

fore easily detected ($\Delta H \approx 6$ mJ). This value should be taken with caution since the recrystallization process is very slow and not yet completed after 25 min, as shown in Fig. 6. This experiment further evidences that such a phase transition may occur at low temperatures and not necessarily upon heating, thanks to the presence of the liquid phase discussed above. Comparing the surface of the diffraction peaks at both SAXS and WAXS, which are related to the amount of crystalline mass, before and after the transition, it can be observed that about twice more crystals are formed 10 min after the transition than at 5 min before the onset of the DSC exotherm. Then, the observed endotherm corresponds in fact to both the transition and a distinct enthalpy of crystallization.

3.4 Packing and electronic density

The SAXS diffraction lines (001, 002) attributed to the fraction with the highest melting point ($h_{1,2}$) are observed at d = 43.8 Å (see Figs. 3, 4). This let us conclude that this 2L structure is formed by trisaturated triacylglycerols representing less than 10% overall, such as SPS and its isomer PSS. The thickness of the β-bilayers expected for SPS and PSS is 43.4 Å and 46.5 Å, respectively [27]. This and the persistence of the line at 4.6 Å on the recording at the slow heating rate (Fig. 4B) make us conclude that the structure associated with the fraction with the highest melting point derives from SPS and is of β 2L type.

The interpretation of the DSC and XRD data associated with the endotherms $h_{3,4,5}$ and $h_{6,7}$ is more difficult. Two β' forms with different melting points [$T_m(\beta'_2) < T_m(\beta'_1)$] are observed in WAXS in this melting domain. In fact, in SAXS recordings, three lines are coupled with these two β' forms. Fig. 3C shows that (i) the β'_2 form is associated with the line at 43.8 Å and endotherm h_6, and (ii) the lines at 35.1 and 48.2 Å contribute to the β'_1 form and endotherms $h_{3,4,5}$. Regarding the attribution of $h_{3,4}$ and $h_{5,6}$, which melt in the range of 20–30 °C and 0–10 °C, respectively, to a triacylglycerol group, it is expected that those correspond to monounsaturated and/or di-unsaturated triacylglycerols, respectively.

The fact that the diffraction peaks of this lowest and highest melting fraction only show distances of about 35 Å is puzzling. This value is too low to correspond to a 2L packing, unless the chain tilt is very important. Taking into account the fatty acid and triacylglycerol composition of lard, we conclude that the observed diffraction at 35 Å does neither correspond to a first order of a 2L packing nor to that of a 3L packing. In spite of a lack of scattering/diffraction in the region of 0.085 $Å^{-1}$, the attribution of the diffraction line observed at 35 Å to the second order of a 3L packing of 70 Å cannot be ruled out (Fig. 4A). A quasi-perfect symmetry of the stacking layer might explain the absence of first order.

In fact, depending on the thermal treatment, the scattering in the domain $0.05\ Å^{-1} \leq q \leq 0.013\ Å^{-1}$ is either U- or V-shaped (arrows in Figs. 3A and 4A). The V-shape present at q centered on 0.08–0.09 Å could also be due to the presence of the first- and second-order diffraction peaks at $q = 0.06$ and $0.12\ Å^{-1}$ of the lamellar structure observed at 35 Å ($q = 0.18\ Å^{-1}$), since they both appear and disappear simultaneously with this peak (in this hypothesis, the stacking period should be 105 Å) (Fig. 4A). An alternative explanation would be that the bump around q = 0.06 Å is a scattering peak, related to crystal sizes, which partly overlap first order of the line at about 35 Å. The U-shape present in the same q range is observed at fast scanning rates and would reflect a less organized structure coming along with broader and weaker diffraction lines.

4 Conclusion

As a summary, we are not able to explain the molecular organization that is reflected by the diffraction peak at 35 Å. Such an organization is made by the monounsaturated TAG (sat., sat., O and sat., O, sat.) that represent about 30% of the fat. Whichever the stacking period, the partial extinction of the first- (and possibly second-) order peaks of a diffraction line at 70 or 105 Å (35 Å) could be related to the specific distribution of the unsaturated fatty acids of lard on the glycerol. Since the diffraction line at 35 Å is not observed for other fats with corresponding fatty acid composition like palm (note that, except for the palmitic/stearic fatty acid ratio, these two fats have similar compositions), one can imagine that a "phase separation" between layers of sat., sat., O and sat., O, sat. triacylglycerols would lead to an alternate structure due to oleic acid esterified in the 2- and 3-position, which might explain the particular electronic density profile.

The fact that structural transitions take place after rapid crystallizations even at low temperatures was related univocally to α to β' prime transition. Taking into account the large difference in molecular volume of the two subcells to which these varieties correspond, the industrial consequence of this polymorphic evolution is the predictable contraction of the fat after fast cooling. Another practical consequence reflected by this work is that lard fractionation would be rather difficult, because the temperature lag between c_1 and c_2 crystallizations only occurs at high cooling rates, resulting in small crystals, while two crystalline varieties are formed simultaneously upon slow cooling in c_2.

Then, we conclude that the coupling of DSC and XRDT allows at least the partial identification of the structures developed during the thermal treatments, whatever the rate, fast or slow, which permits the attribution of the thermal events recorded by DSC. Once this identification has been established, conventional analysis can be undertaken simply using commercially available DSC.

Acknowledgments

We thank L.B.C. for providing lard samples and J.-L. Vandeuvre (CTSCCV, Maisons-Alfort, France) for interest in this work. We thank ACTIA for funding this research and the initial work of D.K. We also thank our group members for their always very fruitful discussions.

References

[1] L. DeMan, V. D'Souza, J. M. DeMan, B. Blackman: Polymorphic stability of some shortenings as influenced by the fatty acid and glyceride composition of the solid phase. *J Am Oil Chem Soc.* 1992, **69**, 246–250.

[2] C. W. Hoerr, D. F. Waugh: Some physical characteristics of rearranged lard. *J Am Oil Chem Soc.* 1955, **32**, 37–41.

[3] L. Kiers: Shortening comprising lard and lipids. US Patent 2733149, 1956.

[4] E. S. Lutton, M. F. Mallery, J. Burgers: Interesterification of lard. *J Am Oil Chem Soc.* 1962, **39**, 233–235.

[5] T. J. Weiss, G. A. Jacobson, L. H. Wiedermann: Reaction mechanics of sodium methoxide treatment of lard. *J Am Oil Chem Soc.* 1961, **38**, 396–399.

[6] D. Rousseau, A. G. Marangoni, K. R. Jeffrey: The influence of chemical interesterification on the physicochemical properties of complex fat systems. 2. Morphology and polymorphism. *J Am Oil Chem Soc.* 1998, **75**, 1833–1839.

[7] K. A. Al Rashood, R. R. A. Abou-Shaaban, E. M. Abdel-Moety, A. Rauf: Compositional and thermal characterization of genuine and randomized lard: A comparative study. *J Am Oil Chem Soc.* 1996, **73**, 303–309.

[8] G. Cornily, M. Le Meste: Flow behavior of lard and of its fractions at 15 °C. Relationship with thermal behavior and chemical composition. *J Texture Studies* 1986, **16**, 383–402.

[9] D. Chapman, A. Crossley, A. C. Davies: The structure of the major component glyceride of cacao butter, and of the major oleodisaturated glyceride of lard. *J Chem Soc.* 1957, 1502–1509.

[10] J. M. N. Marikkar, H. M. Ghazali, Y. B. C. Man, O. M. Lai: Differential scanning calorimetric analysis for determination of some animal fats as adulterants in palm olein. *J Food Lipids* 2003, **10**, 63–79.

[11] O. T. Quimby, R. L. Wille, E. S. Lutton: The glyceride composition of animal fats. *J Am Oil Chem Soc.* 1953, **30**, 186–190.

[12] J. Flanzy, A. Rerat, A. C. Francois: Influence of the structure of the glycerides and the nature of the fatty acids in the feeds on the composition of the depot fat of pigs. *Biophys J.* 1965, **5**, 237–247.

[13] C. Foures: Animal tissues. In: *Manuel des Corps Gras.* Eds: A. Karleskind, J. P. Wolff, Lavoisier ed. Technique et Documentation, Paris (France) 1992, pp. 242–260.

[14] R. Campos, S. S. Narine, A. G. Marangoni: Effect of cooling rate on the structure and mechanical properties of milk fat and lard. *Food Res Int.* 2002, **35**, 971–981.

[15] E. Kaisersberger: Application of heat-flux DSC for the characterization of edible fats and oils. *Anal Proc.* 1990, **27**, 64–65.

[16] G. Keller, F. Lavigne, C. Loisel, M. Ollivon, C. Bourgaux: Investigation of the complex thermal behavior of fats. *J Therm Anal.* 1996, **47**, 1545–1565.

[17] G. Keller, F. Lavigne, L. Forte, K. Andrieux, M. Dahim, C. Loisel, M. Ollivon, C. Bourgaux, P. Lesieur: DSC and X-ray diffraction coupling. *J Therm Anal.* 1998, **51**, 783–791.

[18] F. Lavigne, M. Ollivon: Differential sacnning calorimetry and dynamic X-ray diffraction studies of polymorphic transitions of 2-oleopalmitin. *J Med Cat (Journées Méditéranéennes de Calorimetrie et d'Analyse Thermique), Corte, AFCAT.* 1993, **24**, 237–241.

[19] D. Kalnin, G. Garnaud, H. Amenitsch, M. Ollivon: Monitoring fat crystallization in aerated food emulsions by combined DSC and time-resolved synchrotron X-ray diffraction. *Food Res Int.* 2002, **35**, 927–934.

[20] M. Ollivon: Editorial note: no further information provided.

[21] M. Ollivon, R. Perron: Etude de melanges binaires de triglycerides derives des acides palmitique et stearique. *Chem Phys Lipids.* 1979, **25**, 395–414.

[22] M. Ollivon, R. Perron: Measurements of enthalpies and entropies of unstable crystalline forms of saturated even monoacid triglycerides. *Thermochim Acta* 1982, **53**, 183–194.

[23] V. Gibon, F. Durant, C. Deroanne: Polymorphism and intersolubility of some palmitic, stearic and oleic triglycerides – PPP, PSP and POP. *J Am Oil Chem Soc.* 1986, **63**, 1047–1055.

[24] C. Loisel, G. Keller, G. Lecq, C. Bourgaux, M. Ollivon: Phase transitions and polymorphism of cocoa butter. *J Am Oil Chem Soc.* 1998, **75**, 425–439.

[25] K. Sato: Crystallization behaviour of fats and lipids – a review. *Chem Eng.* 2001, **56**, 2255–2265.

[26] K. Sato, S. Ueno, J. Yan: Molecular interactions and kinetic propertiers of fats. *Prog Lipid Res.* 1999, **38**, 91–116.

[27] D. M. Small: *Handbook of Lipid Research. The Physical Chemistry of Lipids. From Alkanes to Phospholipids.* Plenum Press, New York, NY (USA) 1986.

[28] M. Ollivon, R. Perron: Proprietés physique des corps gras. In: *Manuel des Corps Gras.* Eds. A. Karleskind, J. P. Wolff, Lavoisier ed. Technique et Documentation, Paris (France) 1992, pp. 433–442.

[29] L. H. Wiedermann, T. J. Weiss, G. A. Jacobson, K. F. Mattil: A comparison of sodium methoxide-treated lards. *J Am Oil Chem Soc.* 1961, **38**, 389–395.

[30] C. Grabielle-Madelmond, R. Perron: Calorimetric studies on phospholipid-water systems. *J Colloid Interf Sci.* 1983, **95**, 471–482.

[31] T. C. Huang, H. Toraya, T. N. Blanton, Y. Wu: X-ray-powder diffraction analysis of silver behenate, a possible low-angle diffraction standard. *J Appl Crystallogr.* 1993, **26**, 180–184.

[Received: May 12, 2005; accepted: August 9, 2005]

